

Binary black holes in the pair-instability mass gap

Ugo N. Di Carlo^{1,2,3}, Michela Mapelli^{4,2,3}, Yann Bouffanais^{4,2}, Nicola Giacobbo^{4,2,3},
Alessandro Bressan⁵, Mario Spera^{2,4,6,7} and Francesco Haardt¹

¹*Dipartimento di Scienza e Alta Tecnologia, University of Insubria, Via Valleggio 11, I-22100, Como, Italy*

²*INFN, Sezione di Padova, Via Marzolo 8, I-35131, Padova, Italy*

³*INAF-Osservatorio Astronomico di Padova, Vicolo dell'Osservatorio 5, I-35122, Padova, Italy*

⁴*Dipartimento di Fisica e Astronomia 'G. Galilei', University of Padova, Vicolo dell'Osservatorio 3, I-35122, Padova, Italy*

⁵*Scuola Internazionale Superiore di Studi Avanzati (SISSA), Via Bonomea 265, I-34136 Trieste, Italy*

⁶*Center for Interdisciplinary Exploration and Research in Astrophysics (CIERA), Evanston, IL 60208, USA*

⁷*Department of Physics & Astronomy, Northwestern University, Evanston, IL 60208, USA*

6 November 2019

ABSTRACT

Pair instability (PI) and pulsational PI prevent the formation of black holes (BHs) with mass $\gtrsim 60 M_{\odot}$ from single star evolution. Here, we investigate the possibility that BHs with mass in the PI gap form via stellar mergers and multiple stellar mergers, facilitated by dynamical encounters in young star clusters. We ran 6000 simulations with the direct N-body code NBODY6++GPU coupled with the population synthesis code MOBSE. We find that up to $\sim 5\%$ of all simulated BHs have mass in the PI gap, depending on progenitor's metallicity (this formation channel is more efficient in metal-poor star clusters). BHs with mass in the PI gap are initially single BHs but can efficiently acquire companions through dynamical exchanges. We find that up to $\sim 2\%$ of all binary BH (BBH) mergers have at least one component in the PI mass gap. We predict that up to $\sim 9\%$ of all BBHs detectable by advanced LIGO and Virgo at their design sensitivity have at least one component in the PI mass gap.

Key words: black hole physics – gravitational waves – methods: numerical – galaxies: star clusters: general – stars: kinematics and dynamics – binaries: general

1 INTRODUCTION

The mass function of stellar black holes (BHs) is highly uncertain, as it crucially depends on complex physical processes affecting the evolution and the final fate of massive stars. For a long time, we had to rely on a scanty set of observational data, mostly dynamical mass measurements of compact objects in X-ray binaries (Özel et al. 2010; Farr et al. 2011). In the last three years, gravitational wave (GW) data have completely revolutionised our perspective: ten binary black holes (BBHs) have been observed during the first and the second observing run of the LIGO-Virgo collaboration (LVC, Abbott et al. 2016b; Abbott et al. 2016a; The LIGO Scientific Collaboration & the Virgo Collaboration 2018; Abbott et al. 2019) and we expect that several tens of new BBH mergers will be available by the end of the (currently ongoing) third observing run. GW data will soon provide a Rosetta Stone to decipher the mass function of BBHs.

Thus, it is particularly important to advance our theoretical understanding of BH formation and BH mass function, in order to provide an interpretative key for future

GW data. We currently believe that the mass of a BH depends mainly on the final mass of its progenitor star and on the details of the supernova (SN) explosion (e.g. Heger et al. 2003; Mapelli et al. 2009, 2010, 2013; Belczynski et al. 2010; Fryer et al. 2012; Spera et al. 2015; Limongi & Chieffi 2018). Among all types of SN explosion, pair instability SNe (PISNe) and pulsational pair instability SNe (PPISNe) are expected to leave a strong fingerprint on the mass function of BHs. If the He core mass is larger than $\sim 30 M_{\odot}$, soon after carbon burning when the stellar core temperature reaches $\sim 7 \times 10^8$ K, effective pair production softens the equation of state, leading to a loss of pressure. The stellar core contracts, triggering neon, oxygen and even silicon burning in a catastrophic way, known as pair instability (PI). Stars developing a Helium core mass $64 \leq m_{\text{He}}/M_{\odot} \leq 135$ are thought to be completely disrupted by a PISN, leaving no compact object (Spera & Mapelli 2017). Stars with a smaller Helium core ($32 \lesssim m_{\text{He}}/M_{\odot} \lesssim 64$) undergo pulsational PI: they go through a series of pulsations, losing mass with an enhanced rate, till their cores leave the mass range for PPISNe.

The combination of PISNe and PPISNe leads to a mass gap in the BH mass function between $\sim 60 M_{\odot}$ and ~ 120

M_{\odot} . Both the lower and the upper edge of the mass gap depend on the details of massive star evolution. In particular, the lower edge of the mass gap might span from $\sim 40 M_{\odot}$ up to $\sim 65 M_{\odot}$, depending on the details of PI, stellar evolution and core-collapse SNe (Belczynski et al. 2016; Woosley 2017, 2019; Spera & Mapelli 2017; Giacobbo et al. 2018; Giacobbo & Mapelli 2018; Marchant et al. 2019; Mapelli et al. 2019; Stevenson et al. 2019; Farmer et al. 2019). The upper edge of the gap is even more uncertain. Current LIGO-Virgo data are consistent with a maximum BH mass of $\approx 45 M_{\odot}$, consistent with the existence of a PI mass gap (Abbott et al. 2019).

However, some exotic BH formation channels might populate the PI gap. Hence, the detection of a BH in the mass gap by the LVC would possibly provide a smoking gun for these exotic channels. Primordial BHs (i.e. BHs formed from the collapse of gravitational instabilities in the early Universe, e.g. Carr & Hawking 1974; Carr et al. 2016) could possibly have a mass in the gap. Alternatively, BHs with mass in the gap can form as “second-generation” BHs (Gerosa & Berti 2017), i.e. BHs born from the merger of two smaller BHs.

Finally, Spera et al. (2019) and Di Carlo et al. (2019) proposed a third possible channel to produce BHs in the mass gap. If a massive star with a well-developed Helium core merges with a non-evolved companion (a main sequence or an Hertzsprung-gap star), it might give birth to an evolved star with an over-sized hydrogen envelope. If the Helium core remains below $\sim 32 M_{\odot}$ and the star collapses to a BH before growing a much larger core and before losing a significant fraction of its envelope, the final BH might be in the PI mass gap.

If a second-generation BH or a BH born from stellar merger form in the field, they remain single objects and we do not expect to observe them in a BBH merger. In contrast, if they form in a dense stellar cluster they might capture a new companion through a dynamical exchange, possibly becoming a BBH (Miller & Hamilton 2002; Di Carlo et al. 2019; Rodriguez et al. 2019; Gerosa & Berti 2019). Here, we focus on BHs in the PI gap formed from stellar mergers and we estimate their mass range, merger efficiency and detection probability.

2 METHODS

The simulations discussed in this paper were done using the same code and methodology as described in Di Carlo et al. (2019). In particular, we use the direct summation N-Body code NBODY6++GPU (Wang et al. 2015) coupled with the new population synthesis code MOBSE (Mapelli et al. 2017; Giacobbo et al. 2018; Giacobbo & Mapelli 2018). MOBSE includes up-to-date prescriptions for massive star winds, for core-collapse SN explosions and for PISNe and PPISNe.

Here, we simulate a large set of young star clusters (SCs). Young SCs are thought to be the nursery of massive stars in the local Universe (see e.g. Lada & Lada 2003; Portegies Zwart et al. 2010). Unlike globular clusters, young SCs are asymmetric, rather clumpy systems. Thus, we model them with fractal initial conditions (Küpper et al. 2011), to mimic initial clumpiness (Goodwin & Whitworth 2004). The level of fractality is decided by the parameter D (where

Table 1. Initial conditions.

Set	N_{sim}	$M_{\text{SC}} [M_{\odot}]$	Z	f_{bin}	D
Z0002	1×10^3	$0.1 - 3 \times 10^4$	0.0002	0.4	1.6
Z002	4×10^3	$0.1 - 3 \times 10^4$	0.002	0.4	1.6, 2.3
Z02	1×10^3	$0.1 - 3 \times 10^4$	0.02	0.4	1.6

Column 1: Name of the simulation set. Set Z002 is the sum of all the simulations already presented in Di Carlo et al. (2019), while sets Z02 and Z0002 are new sets. Column 2: Number of runs performed per each set. Column 3: total mass of SCs (M_{SC}). Column 4: metallicity (Z). Column 5: fraction of stars that are initially in binary systems (f_{bin}). Column 6: fractal dimension (D). Half of the simulations in set Z002 have $D = 1.6$ and the other half have $D = 2.3$ (see Di Carlo et al. 2019). In this analysis, we put them together because the results we present here do not depend on fractality.

$D = 3$ means homogeneous distribution of stars). In this work, we adopt $D = 1.6$ (high-fractality runs) and $D = 2.3$ (low-fractality runs).

In this work, we have simulated 6×10^3 fractal young SCs. The initial conditions of the simulations presented in this paper are summarized in Table 1. The total mass M_{SC} of each SC (ranging from $1000 M_{\odot}$ to $30000 M_{\odot}$) is drawn from a distribution $dN/dM_{\text{SC}} \propto M_{\text{SC}}^{-2}$, as the embedded SC mass function described in Lada & Lada (2003). Thus, the mass distribution of our simulated SCs mimics the mass distribution of SCs in Milky Way-like galaxies. We choose the initial SC half mass radius r_h according to the Marks & Kroupa relation (Marks et al. 2012).

We consider three different metallicities: $Z = 0.0002$, 0.002 and 0.02 (approximately 1/100, 1/10 and 1 Z_{\odot}). For $Z = 0.002$ we run two sub-sets of simulations, one with $D = 1.6$ and the other with $D = 2.3$. For $Z = 0.0002$ and $Z = 0.02$ we just run one set with $D = 1.6$ (after testing that the D parameter does not affect our results significantly). The simulations with $Z = 0.002$ are the same as presented in Di Carlo et al. (2019), while the simulations with $Z = 0.02$ and $Z = 0.0002$ are two new sets of runs.

The stars in the simulated SCs follow a Kroupa (2001) initial mass function, with minimum mass $0.1 M_{\odot}$ and maximum mass $150 M_{\odot}$. We assume an initial binary fraction $f_{\text{bin}} = 0.4$. The orbital periods, eccentricities and mass ratios of binaries are drawn from Sana et al. (2012). We simulate each star cluster for 100 Myr in a rigid tidal field corresponding to the Milky Way tidal field at the orbit of the Sun. We refer to Di Carlo et al. (2019) for further details on the code and on the initial conditions.

3 RESULTS

From our simulations, we extract information on BHs with mass in the PI gap, between 60 and $150 M_{\odot}$ (given the uncertainties on the edges of the mass gap, we make a conservative assumption for both the lower and the upper edge of the mass gap). In Di Carlo et al. (2019), we have already discussed the properties of BHs that form from stars with $Z = 0.002$, have mass in the PI gap and merge with other BHs in less than a Hubble time. Here, we extend our study

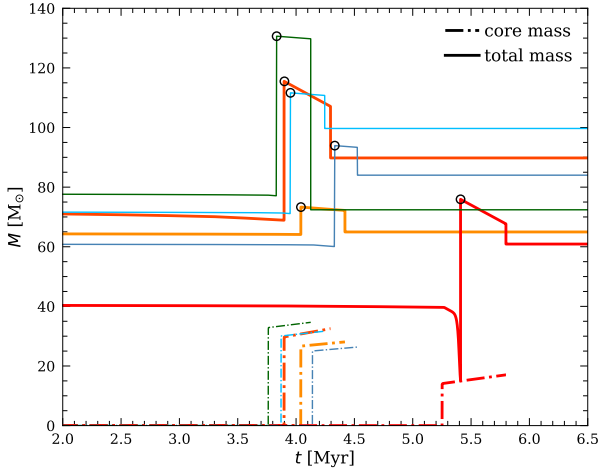


Figure 1. Evolution of the total mass (solid lines) and the core mass (dot-dashed lines) of the progenitors of a sample of BHs with mass in the gap. The black circle marks the time of the merger with a companion star. Thick (red, orange and yellow) lines are stars which end up in merging BBHs, while thin (light blue, blue and green) lines become single BHs.

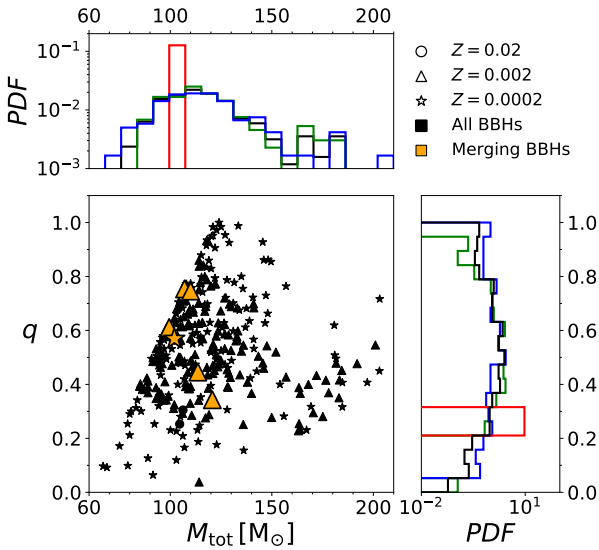


Figure 2. Mass ratio $q = M_2/M_1$ versus total mass $M_{\text{tot}} = M_1 + M_2$ of BHs with mass in the gap that are members of BBHs by the end of the simulations. Circles, triangles and stars refer to $Z = 0.02$, 0.002 and 0.0002 , respectively. Orange and black symbols refer to BBHs merging within a Hubble time and to all BBHs, respectively. Marginal histograms show the distribution of q (on the y -axis) and M_{tot} (on the x -axis). The black histograms show the distributions for all the simulations, while the blue, green and red histograms refer to $Z = 0.0002$, 0.002 and 0.02 , respectively.

to other progenitor’s metallicities ($Z = 0.02$ and 0.0002) and we investigate the main properties of all BHs that form in the PI mass gap from our dynamical simulations.

3.1 Formation channels of BHs in the gap

The vast majority of BHs with mass in the PI gap that form in our simulation originates from the merger of an evolved

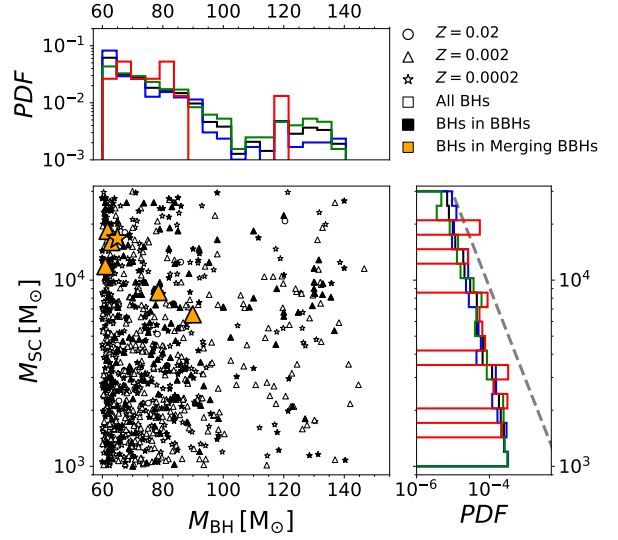


Figure 3. Mass of the host star cluster (M_{SC}) versus the mass M_{BH} of a BH in the PI gap. Marginal histograms show the distribution of M_{SC} (on the y -axis) and M_{BH} (on the x -axis). Orange and black filled symbols refer to BBHs merging within a Hubble time and to all BBHs, respectively. Open symbols show single BHs. The black histograms show the distributions for all the simulations, while the blue, green and red histograms refer to $Z = 0.0002$, 0.002 and 0.02 , respectively. The dashed line shows the mass function of M_{SC} in our simulation set ($dN/dM_{\text{SC}} \propto M_{\text{SC}}^{-2}$).

star (with a developed Helium core of mass $\approx 15 - 30 M_{\odot}$) and a main sequence companion. The merger is generally triggered by dynamical perturbations. In several cases, the evolved star is the result of multiple mergers between other stars, facilitated by the dense dynamical environment. This process of multiple mergers occurring in a very short time span is known as runaway collision and was already discussed in several papers (see e.g. Portegies Zwart & McMillan 2002; Portegies Zwart et al. 2004; Giersz et al. 2015; Mapelli 2016; Gieles et al. 2018).

Figure 1 shows the evolution of six stellar progenitors of BHs in the PI mass gap. Three of these BHs become members of BBHs and merge within a Hubble time, while the other three objects leave single BHs. We find no significant difference between the formation channel of merging BBHs in the PI mass gap and that of single BHs or non-merging BBHs with mass in the PI gap.

The stars shown in Figure 1 undergo a merger with a main-sequence companion in their late evolutionary stages ($\sim 4 - 6$ Myr), when they are Hertzsprung gap or core Helium burning stars. We assume that the mass of the merger product is the sum of the mass of the two stars. The merger products are not significantly rejuvenated, because they already developed a He core. They are evolved based on their mass and are subject to stellar winds, depending on their metallicity. Their final He core is $\sim 17 - 32 M_{\odot}$ (below the PPISN/PISN gap), while their hydrogen envelope is oversized with respect to single star evolution, because of the merger.

In all the simulations, the post-merger star evolves for $t_{\text{post-merg}} = t_{\text{He}} + t_{\text{C}} + t_{\text{Ne}} + t_{\text{O}} + t_{\text{Si}} \sim t_{\text{He}}$, where $t_{\text{post-merg}}$

is the time remaining to collapse, while t_{He} , t_{C} , t_{Ne} , t_{O} and t_{Si} are the timescale of Helium, Carbon, Neon, Oxygen and Silicon burning, respectively. During $t_{\text{post-merg}}$, the star converts a mass $\Delta M_{\text{He}} \sim \dot{M}_{\text{He}} t_{\text{post-merg}}$, where

$$\dot{M}_{\text{He}} \lesssim 2 \times 10^{-5} M_{\odot} \text{ yr}^{-1} \left(\frac{L_*}{10^6 L_{\odot}} \right) \left(\frac{6.3 \times 10^{18} \text{ erg g}^{-1}}{\eta_{\text{CNO}}} \right) \left(\frac{0.5}{X} \right). \quad (1)$$

In equation 1, L_* is the stellar luminosity, X is the hydrogen fraction and η_{CNO} is the efficiency of mass-to-energy conversion during the CNO cycle (e.g. Prialnik 2000).

If the final mass of the Helium core $M_{\text{He},\text{f}} = M_{\text{He}} + \Delta M_{\text{He}} < 32 M_{\odot}$, where M_{He} is the mass of the Helium core before the last stellar merger, then the star with an oversized hydrogen envelope can avoid PI and directly collapses to a BH, possibly with mass $> 60 M_{\odot}$. This is just an order of magnitude estimation, more refined calculations would require a hydrodynamical simulation to follow the merger (see e.g. Gaburov et al. 2010) and a stellar-evolution code to integrate nuclear burning and stellar evolution (Bressan et al., in preparation).

The efficiency of BH formation with mass in the gap depends on stellar metallicity. More than $\sim 5\%$ of all simulated BHs have mass in the gap at metallicity $Z = 0.0002$ ($\sim 1/100$ solar), which decreases to approximately $\sim 1\%$ for $Z = 0.002$ and drops to nearly zero at $Z = 0.02$ (see Table 2). This difference clearly originates from stellar winds: when stellar winds are efficient, it is extremely difficult to merge two stars with a large hydrogen envelope, because massive stars lose their envelope almost completely in few Myr.

Once they form, BHs with mass in the gap are quite efficient in acquiring companions: $\sim 11\%$ and $\sim 9\%$ of all BBHs have at least one member with mass in the PISN gap at $Z = 0.0002$ and $Z = 0.002$, respectively. This is quite expected, because these BHs are significantly more massive than the other BHs and stars in the SCs, and dynamical exchanges favour the formation of more massive binaries, which are more energetically stable (see e.g. Ziosi et al. 2014; Mapelli 2016).

If we consider only BBHs merging within a Hubble time (14 Gyr) due to GW emission, only $\sim 0.6\%$ and $\sim 2\%$ of them have at least one BH in the PI gap at $Z = 0.0002$ and $Z = 0.002$, respectively. We find only six merging BBHs with a BH in the PI gap, hence these percentages might be significantly affected by stochastic fluctuations. These BBHs merge after being ejected from their parent young SC. Finally, we find no merging BBHs with members in the PI gap at solar metallicity.

None of the BBHs in our simulations hosts a second-generation BH (i.e. a BH that forms from the merger of two BHs). The low escape velocity from our SCs (up to few km s^{-1} in the most massive SCs) prevents second-generation BHs from remaining inside the cluster: all of them are ejected and cannot acquire a new companion. In contrast, in massive SCs (like globular clusters and nuclear star clusters) second-generation BHs have a significantly higher chance of remaining inside their parent cluster and acquiring a companion (see e.g. Miller & Hamilton 2002; Colpi et al. 2003; Antonini & Rasio 2016; Rodriguez et al. 2019).

It is important to highlight several caveats inherent with our analysis. First, MOBSE assumes that no mass is lost

Table 2. Fraction of BHs, BBHs and merging BBHs with mass in the PI gap.

Z	$f_{\text{PI, BHs}}$	$f_{\text{PI, BBHs}}$	$f_{\text{PI, GW}}$	$p_{\text{det}}^{\text{PI}}$
0.0002	5.5 %	11.5 %	0.6 %	2.6 %
0.002	1.4 %	9.0 %	2.2 %	8.9 %
0.02	0.2 %	0.6 %	0.0 %	0 %

Column 1 (Z): progenitor metallicity; column 2 ($f_{\text{PI, BHs}}$): percentage of BHs with mass in the PI gap with respect to all simulated BHs at a given Z ; column 3 ($f_{\text{PI, BBHs}}$): percentage of BBHs that have at least one member with mass in the PI gap with respect to all BBHs at a given Z formed by the end of the simulations. column 4 ($f_{\text{PI, GW}}$): percentage of merging BBHs that have at least one member with mass in the PI gap with respect to all merging BBHs at a given Z (a merging BBH is defined as a BBH which merges in less than a Hubble time by GW emission); column 5 ($p_{\text{det}}^{\text{PI}}$): percentage of detectable BBH mergers that have at least one member with mass in the PI gap with respect to all detectable BBH mergers at a given Z ; see equation 3.

during the merger while hydrodynamical simulations have shown that mass ejecta can represent up to ~ 25 per cent of the total mass Gaburov et al. (2010). Furthermore, the polynomial fitting formulas implemented in MOBSE might be inaccurate to describe the final evolution of such post-merger massive stars. In a follow-up work, we will evolve our post-collision models with a stellar evolution code, to check any deviations from MOBSE. In addition, we assume that the final hydrogen envelope entirely collapses to a BH. This final outcome depends on the final binding energy of the envelope (see e.g. Sukhbold et al. 2016 for a discussion). Finally, we model PPISNe with a fitting formula (Spera & Mapelli 2017) to the models by Woosley (2017). However, the models by Woosley (2017) are suited for stars following regular single stellar evolution, that could be significantly different from merger products.

3.2 Mass distribution

Figure 2 shows the mass ratio $q = M_2/M_1$ (where $M_1 > M_2$) and the total mass $M_{\text{tot}} = M_1 + M_2$ of all BBHs that have at least one member in the PI gap. We form BHs with masses in the entire range of the PI gap between $\sim 60 - 150 M_{\odot}$, with a preference for masses around $60 - 70 M_{\odot}$.

Values of mass ratios in the range $q \sim 0.4 - 0.6$ are the most likely, but we find binaries with q as low as ~ 0.04 and as high as ~ 1 . The binary with the smallest value of q has secondary mass $M_2 \sim 4.2 M_{\odot}$. The largest secondary mass is $M_2 \sim 110 M_{\odot}$. Overall, binaries hosting a BH with mass in the gap have lower mass ratios than other BBHs (see Figure 7 of Di Carlo et al. 2019, where we show that the vast majority of BBHs in young SCs have $q \sim 0.9 - 1$).

Figure 3 shows the mass of the host SC as a function of the mass of BHs in the PI gap (here we include also BHs that remain single). BHs in the mass gap form more efficiently in massive young SCs, where dynamics is more important. All the six merging BBHs are hosted in star clusters with $M_{\text{SC}} > 6000 M_{\odot}$, among the most massive young SCs in our sample.

3.3 Merger and detection efficiency

We find that only $\sim 0 - 2$ % of all merging BBHs have at least one member with mass in the PI gap, depending on metallicity. However, these systems are significantly more massive than other merging BBHs, thus they have a higher detection chance. To properly take into account these selection effects, we followed a similar approach as in [Finn & Chernoff \(1993\)](#), [Dominik et al. \(2015\)](#) and [Bouffanaïs et al. \(2019\)](#).

We associate to each mock source (in our catalogue of 412 merging BBHs) the optimal signal-to-noise ratio (SNR) ρ_{opt} that corresponds to the case where the source is optimally oriented and located in the sky. Since real-life sources have different orientations and locations, we then reweigh the SNR as $\rho = \omega \times \rho_{opt}$, where ω takes randomly generated values between 0 and 1, and the probability of detecting a source is given by

$$p_{det} = 1 - F_{\omega}(\rho_{thr}/\rho_{opt}). \quad (2)$$

In this equation, F_{ω} is the cumulative function of ω and ρ_{thr} is a detection threshold. We use $\rho_{thr} = 8$, that was shown to be a good approximation for a network of detectors ([Abadie et al. 2010](#); [Abbott et al. 2016c](#)). We used the software PyCBC ([Dal Canton et al. 2014](#); [Usman et al. 2016](#)) to generate both the waveforms (IMRPhenomB with zero spins) and the noise power spectral densities of advanced LIGO at design sensitivity ([Abbott et al. 2018](#)), and the package gwdet ([Gerosa 2019](#)) to evaluate the function F_{ω} .

As redshift is not provided in our simulations, we marginalised p_{det} over redshift z , by averaging the values obtained with a sample of 10^4 sources where z is distributed uniformly in comoving volume between 0 and 1 (corresponding roughly to the detection horizon of advanced LIGO) while keeping the other parameters constant.

Finally, to obtain the probability of detecting a source with at least one component in the PI mass gap, we computed the following quantity

$$p_{det}^{PI} = \sum_{i \in PI} p_{det}^i / \sum_j p_{det}^j, \quad (3)$$

where the sum in the numerator is done only over sources where at least one component lies in the mass gap while the sum in the denominator is done over all sources in our catalogue of merging BBHs. In this preliminary work, we calculate p_{det}^{PI} per each metallicity separately, because we do not assume a metallicity evolution with redshift. In a follow-up paper ([Santoliquido et al.](#), in preparation), we will model metallicity and redshift evolution self-consistently.

We find $p_{det}^{PI} = 0 - 9$ %, depending on metallicity (see the last column of [Table 2](#)). This means that, under our assumptions, up to 9 % of all BBHs detected by LIGO-Virgo at design sensitivity have at least one component in the PI mass gap.

4 CONCLUSIONS

Pair instability (PI) and pulsational PI prevent the formation of BHs with mass between ~ 60 and $\sim 150 M_{\odot}$ from single stellar evolution. However, binary evolution processes (such as stellar mergers) and dynamical processes might allow the formation of BHs with masses in the gap.

Here, we investigate the possibility that BHs with mass in the gap form through stellar mergers and multiple stellar mergers in young SCs. The merger between an evolved star (a giant with a well developed Helium core) and a main sequence star can give birth to a BH with mass in the gap, provided that the star collapses before its Helium core grows above $\sim 32 M_{\odot}$. In our simulations, these stellar mergers are facilitated by the SC environment: dynamical encounters perturb a binary star, affecting its orbital properties and increasing the probability of a merger between its components. Some massive stars even undergo runaway collisions: they go through multiple mergers over few Myrs. When a BH with mass in the PI gap forms in this way, it is initially a single object. If it remains in the SC, it can acquire a new companion through dynamical exchanges.

In contrast, BHs that form via stellar mergers in the field remain single BHs. Moreover, BHs with masses $> 60 M_{\odot}$ are much harder to form in isolated binaries, because dissipative mass transfer peels-off the primary before the merger. Dynamical encounters perturb the binary and induce a fast merger without episodes of mass transfer.

We have investigated the formation and the dynamical evolution of BHs with masses in the gap through 6000 direct N-body simulations of young SCs with metallicity $Z = 0.0002, 0.002$ and 0.02 , respectively. At the end of our simulations, ~ 5.5 %, ~ 1.3 % and ~ 0.2 % of all BHs have mass in the PI gap for metallicity $Z = 0.0002, 0.002$ and 0.02 , respectively. Metal-poor stars are more efficient in producing these BHs, because they lose less mass by stellar winds. In our simulations, we do not include prescriptions for BH spins, because the connection between the spin of the progenitor star and the spin of the BH is highly uncertain (see e.g. [Heger et al. 2005](#); [Lovegrove & Woosley 2013](#); [Belczynski et al. 2017](#); [Qin et al. 2018, 2019](#); [Fuller et al. 2019](#); [Fuller & Ma 2019](#)). We can speculate that stellar mergers spin up the progenitor stars, but we cannot tell whether this spin-up translates into a higher BH spin.

It is worth mentioning that the treatment of the merger of two stars in our simulations is very simplified: we assume no mass loss and no chemical mixing during the merger and we require that the merger product reaches hydro-static equilibrium instantaneously. The merger product is rejuvenated according to [Hurley et al. \(2002\)](#) prescriptions. These assumptions are quite crude. Hydrodynamical simulations of the stellar merger are required in order to have a better understanding of the final outcome. Thus, our results should be regarded as a strong upper limit to the formation of BHs in the PI mass gap via stellar mergers.

In our simulations, several BHs with masses in the gap end up forming a BBH through dynamical exchanges. BBHs having at least one component in the mass gap are ~ 12 %, ~ 9 % and ~ 1 % of all BBHs in our simulations, for metallicity $Z = 0.0002, 0.002$ and 0.02 , respectively. Thus, BHs with masses in the gap are quite efficient in forming BBHs. The total masses of these BBHs are typically around $\sim 90 - 130 M_{\odot}$ and the most likely mass ratios are $\sim 0.4 - 0.6$.

In our simulations, ~ 2.4 % (~ 0.5 %) of all BBHs merging within a Hubble time have at least one component in the mass gap for metallicity $Z = 0.002$ ($Z = 0.0002$). We find no merging BBHs in the mass gap at solar metallicity. Merging BBHs in the mass gap form preferentially in the most massive SCs we simulate ($M_{SC} \geq 6000 M_{\odot}$). Since merging

BBHs in the mass gap form through dynamical exchanges, their spins will be isotropically oriented with respect to the orbital angular momentum of the binary system.

Finally, we calculate the probability that advanced LIGO and Virgo at design sensitivity detect the merger of BBHs in the mass gap. We predict that up to $\sim 9\%$ of all BBH mergers detected by LIGO and Virgo at design sensitivity have at least one component in the PI mass gap. If the proposed mechanism to form BHs in the mass gap is actually at work, the LIGO-Virgo collaboration might be able to witness these events in the next few years.

ACKNOWLEDGMENTS

We thank Mark Gieles, the internal P&P reviewer of the LVC. UNDC acknowledges financial support from Università degli Studi dell'Insubria through a Cycle 33rd PhD grant. MM and YB acknowledge financial support by the European Research Council for the ERC Consolidator grant DEMOBLACK, under contract no. 770017. MS acknowledges funding from the European Union's Horizon 2020 research and innovation programme under the Marie-Sklodowska-Curie grant agreement No. 794393. AB acknowledges support by PRIN MIUR 2017 prot.20173ML3WW 002 "Opening the ALMA window on the cosmic evolution of gas, stars and supermassive black holes". This work benefited from support by the International Space Science Institute (ISSI), Bern, Switzerland, through its International Team programme ref. no. 393 *The Evolution of Rich Stellar Populations & BH Binaries* (2017-18).

REFERENCES

- Abadie J., et al., 2010, *Classical and Quantum Gravity*, **27**, 173001
- Abbott B. P., et al., 2016a, *Physical Review X*, **6**, 041015
- Abbott B. P., et al., 2016b, *Phys. Rev. Lett.*, **116**, 061102
- Abbott B. P., et al., 2016c, *Astrophys. J.*, **833**, L1
- Abbott B. P., et al., 2018, *Living Rev. Rel.*, **21**, 3
- Abbott B. P., Abbott R., Abbott T. D., Abraham S., Acernese F., et al. 2019, *ApJ*, **882**, L24
- Antonini F., Rasio F. A., 2016, *ApJ*, **831**, 187
- Belczynski K., Bulik T., Fryer C. L., Ruiter A., Valsecchi F., Vink J. S., Hurley J. R., 2010, *ApJ*, **714**, 1217
- Belczynski K., et al., 2016, *A&A*, **594**, A97
- Belczynski K., et al., 2017, arXiv e-prints, p. [arXiv:1706.07053](https://arxiv.org/abs/1706.07053)
- Bouffanais Y., Mapelli M., Gerosa D., Di Carlo U. N., Giacobbo N., Berti E., Baibhav V., 2019, arXiv e-prints, p. [arXiv:1905.11054](https://arxiv.org/abs/1905.11054)
- Carr B. J., Hawking S. W., 1974, *MNRAS*, **168**, 399
- Carr B., Kühnel F., Sandstad M., 2016, *Phys. Rev. D*, **94**, 083504
- Colpi M., Mapelli M., Possenti A., 2003, *ApJ*, **599**, 1260
- Dal Canton T., et al., 2014, *Phys. Rev.*, D90, 082004
- Di Carlo U. N., Giacobbo N., Mapelli M., Pasquato M., Spera M., Wang L., Haardt F., 2019, *MNRAS*, **487**, 2947
- Dominik M., et al., 2015, *ApJ*, **806**, 263
- Farmer R., Renzo M., de Mink S. E., Marchant P., Justham S., 2019, arXiv e-prints, p. [arXiv:1910.12874](https://arxiv.org/abs/1910.12874)
- Farr W. M., Sravan N., Cantrell A., Kreidberg L., Bailyn C. D., Mandel I., Kalogera V., 2011, *ApJ*, **741**, 103
- Finn L. S., Chernoff D. F., 1993, *Phys. Rev.*, D47, 2198
- Fryer C. L., Belczynski K., Wiktorowicz G., Dominik M., Kalogera V., Holz D. E., 2012, *ApJ*, **749**, 91
- Fuller J., Ma L., 2019, *ApJ*, **881**, L1
- Fuller J., Piro A. L., Jermyn A. S., 2019, *MNRAS*, **485**, 3661
- Gaburov E., Lombardi Jr. J. C., Portegies Zwart S., 2010, *MNRAS*, **402**, 105
- Gerosa D., 2019, gwdet:Detectability of gravitational-wave signals from compact binary coalescences, doi:doi.org/10.5281/zenodo.889966.
- Gerosa D., Berti E., 2017, *Phys. Rev. D*, **95**, 124046
- Gerosa D., Berti E., 2019, arXiv e-prints, p. [arXiv:1906.05295](https://arxiv.org/abs/1906.05295)
- Giacobbo N., Mapelli M., 2018, *MNRAS*, **480**, 2011
- Giacobbo N., Mapelli M., Spera M., 2018, *MNRAS*, **474**, 2959
- Gieles M., et al., 2018, *MNRAS*, **478**, 2461
- Giersz M., Leigh N., Hupki A., Lützgendorf N., Askar A., 2015, *MNRAS*, **454**, 3150
- Goodwin S. P., Whitworth A. P., 2004, *A&A*, **413**, 929
- Heger A., Fryer C. L., Woosley S. E., Langer N., Hartmann D. H., 2003, *ApJ*, **591**, 288
- Heger A., Woosley S. E., Spruit H. C., 2005, *ApJ*, **626**, 350
- Hurley J. R., Tout C. A., Pols O. R., 2002, *MNRAS*, **329**, 897
- Kroupa P., 2001, *MNRAS*, **322**, 231
- Küpper A. H. W., Maschberger T., Kroupa P., Baumgardt H., 2011, *MNRAS*, **417**, 2300
- Lada C. J., Lada E. A., 2003, *ARA&A*, **41**, 57
- Limongi M., Chieffi A., 2018, *ApJS*, **237**, 13
- Lovegrove E., Woosley S. E., 2013, *ApJ*, **769**, 109
- Mapelli M., 2016, *MNRAS*, **459**, 3432
- Mapelli M., Colpi M., Zampieri L., 2009, *MNRAS*, **395**, L71
- Mapelli M., Ripamonti E., Zampieri L., Colpi M., Bressan A., 2010, *MNRAS*, **408**, 234
- Mapelli M., Zampieri L., Ripamonti E., Bressan A., 2013, *MNRAS*, **429**, 2298
- Mapelli M., Giacobbo N., Ripamonti E., Spera M., 2017, *MNRAS*, **472**, 2422
- Mapelli M., Spera M., Montanari E., Limongi M., Chieffi A., Giacobbo N., Bressan A., 2019, arXiv e-prints, p. [arXiv:1909.01371](https://arxiv.org/abs/1909.01371)
- Marchant P., Renzo M., Farmer R., Pappas K. M. W., Taam R. E., de Mink S. E., Kalogera V., 2019, *ApJ*, **882**, 36
- Marks M., Kroupa P., Dabringhausen J., Pawlowski M. S., 2012, *MNRAS*, **422**, 2246
- Miller M. C., Hamilton D. P., 2002, *MNRAS*, **330**, 232
- Özel F., Psaltis D., Narayan R., McClintock J. E., 2010, *ApJ*, **725**, 1918
- Portegies Zwart S. F., McMillan S. L. W., 2002, *ApJ*, **576**, 899
- Portegies Zwart S. F., Baumgardt H., Hut P., Makino J., McMillan S. L. W., 2004, *Nature*, **428**, 724
- Portegies Zwart S. F., McMillan S. L. W., Gieles M., 2010, *ARA&A*, **48**, 431
- Prialnik D., 2000, An Introduction to the Theory of Stellar Structure and Evolution
- Qin Y., Fragos T., Meynet G., Andrews J., Sørensen M., Song H. F., 2018, *A&A*, **616**, A28
- Qin Y., Marchant P., Fragos T., Meynet G., Kalogera V., 2019, *ApJ*, **870**, L18
- Rodriguez C. L., Zevin M., Amaro-Seoane P., Chatterjee S., Kremer K., Rasio F. A., Ye C. S., 2019, arXiv e-prints, p. [arXiv:1906.10260](https://arxiv.org/abs/1906.10260)
- Sana H., et al., 2012, *Science*, **337**, 444
- Spera M., Mapelli M., 2017, *MNRAS*, **470**, 4739
- Spera M., Mapelli M., Bressan A., 2015, *MNRAS*, **451**, 4086
- Spera M., Mapelli M., Giacobbo N., Trani A. A., Bressan A., Costa G., 2019, *MNRAS*, **485**, 889
- Stevenson S., Sampson M., Powell J., Vigna-Gómez A., Neijssel C. J., Szécsi D., Mandel I., 2019, *ApJ*, **882**, 121
- Sukhbold T., Ertl T., Woosley S. E., Brown J. M., Janka H. T., 2016, *ApJ*, **821**, 38
- The LIGO Scientific Collaboration the Virgo Collaboration 2018, preprint, ([arXiv:1811.12907](https://arxiv.org/abs/1811.12907))

- Usman S. A., et al., 2016, *Class. Quant. Grav.*, 33, 215004
Wang L., Spurzem R., Aarseth S., Nitadori K., Berczik P.,
Kouwenhoven M. B. N., Naab T., 2015, *MNRAS*, 450, 4070
Woosley S. E., 2017, *ApJ*, 836, 244
Woosley S. E., 2019, *ApJ*, 878, 49
Ziosi B. M., Mapelli M., Branchesi M., Tormen G., 2014, *MNRAS*,
441, 3703